Journal of the Oceanographical Society of Japan
Vol. 28, pp. 187 to 202, October, 1972

A Field Study of the Development of Wind-waves*

Part 1. The Experiment

Keisuke TAIRA**

Abstract: This paper presents the results of observation on the development of wind-waves which were generated in a lake water about 420 cm deep with a fetch 12 km long. Measurements of surface elevation were carried out at the end of an observational pier where the water depth was 80 cm. The wave momentum flux, i.e., the growth rate of the wave momentum, was estimated from both significant waves and power spectral densities for the wave records. The values obtained by the two ways accorded fairly well and they were 5~7 % as large as the wind stress measured simultaneously. The exponential growth rate of spectral densities for a frequency component was in good accord with that observed by SNYDER and COX (1966) and by others. If these growth rates are applied to all the components of the spectrum, the wave momentum flux must exceed the wind stress. This cannot explain the experimental results nor can be physically accepted. The difference of spectral densities between the two successive runs showed that the increase of spectral densities was limited in several bands of frequency. The phenomena are discussed in relation with the 'overshoot-undershoot effects' studied by BARNETT and SUTHERLAND (1968).

Observational results suggest that the spectral growth of a certain component is closely related to the spectral densities of other components. Energy exchange among componented waves has not been considered in the theories for generation and development of wind-waves established by Phillips, Miles and others.

New generation mechanism suggested by LONGUET-HIGGINS (1969) was found to be able to describe the observed growth rates of the form $\Phi(f)=\{\gamma(f)(t-t_f)\}^2$: the spectral density $\Phi(f)$ was proportional to the square of duration t. However, the mechanism can not explain the overshoot-undershoot effects peculiar to the equilibrium spectrum of wind-waves.

Three frequencies characterizing the discrete distributions of frequency bands where spectral densities increased were examined and three waves corresponding to these frequencies were found to be satisfying the resonance conditions for the 'wave-wave interactions' among three sinusoidal wave trains as studied by PHILLIPS (1960), LONGUET-HIGGINS (1962) and BENNY (1962). The interactions are suggested to predict well both the spectral growth proportional to squares of duration and the ceaseless oscillations of spectral densities in an equilibrium spectrum.

1. Introduction

The wind blowing over the sea surface imparts its momentum to water and induces the wind-waves. This fascinating process of generation and development of wind-waves has been studied theoretically and observationally by many investigators. However, recently LONGUET-HIGGINS (1969) has said "It is now evident that the mechanism mainly responsible for the most rapid stage of sea waves under the action of the wind still remains to be found."

This paper presents some observational results of the development of wind-waves generated in a lake water. After comparing these results with some theories and observations, the process of 'wave-wave interactions' (cf. LONGUET-HIGGINS 1962) is suggested to be the most responsible mechanism for the rapid growth of wind-waves.

* Received July 4, 1972
** Ocean Research Institute University of Tokyo
Nakano, Tokyo, 164 Japan

2. Background

Some previous works are reviewed from a viewpoint of the momentum conservation. With a wave train of surface waves $\zeta=a\cos(kx+\sigma t)$, there is associated both an energy density $E=\rho g\overline{\zeta^2}=\frac{1}{2}\rho g a^2$, and a horizontal momentum density M, related E by the simple equation

$$M=E/c \qquad (1)$$

where $c=\sigma/k$ denotes the phase velocity and x-axis is taken in the direction of wave propagation. Wave momentum flux τ_w of the wave train is represented by

$$\tau_w=\frac{dM}{dt} \qquad (2)$$

Ocean waves generated by the action of the highly turbulent winds are generally random and irregular. A significant wave has been introduced in order to represent the energy of such ocean waves. From the duration graph of the growth of the significant waves, the wave momentum flux is estimated by the equation

$$\tau_w=\frac{d}{dt}\left(\frac{E}{c}\right)=\frac{1}{c}\frac{dE}{dt}-\frac{E}{c^2}\frac{dc}{dt} \qquad (3)$$

By this method, STARR (1947) found $\tau_w\sim 0.1\tau_a$, where τ_a is the wind stress, for a duration graph of SVERDRUP and MUNK (1947). STEWART (1961) estimated to be $\tau_w\sim 0.2\,\tau_a$ and KORVIN-KROUKOVSKY (1965) found $\tau_w=(0.06\sim 0.07)\,\tau_a$.

On the other hand, the energy of ocean waves is strictly expressed by a spectral density $F(\sigma)$ as

$$E=\rho g\overline{\zeta^2}=\rho g\int_0^\infty F(\sigma)d\sigma \qquad (4)$$

Wave momentum flux is described by

$$\tau_w=\rho g\int_0^\infty \frac{1}{c(\sigma)}\frac{dF(\sigma)}{dt}d\sigma \qquad (5)^*$$

By the method TAIRA (1971a) has estimated that $\tau_w\leqq 0.16\,\tau_n$ in his observations. HAMADA, SHIBAYAMA and KATO (1966) also found $\tau_w=0.16\,\tau_a$ in their experiment carried out in a wave-tank.

The wave momentum flux calculated by (3) or (5) shows the increase of the momentum of waves which remain after decaying under the action of viscosity or by breaking. Any kind of fluid motion is caused by the momentum lost by breaking has been little known. LONGUET-HIGGINS (1969) suggests that the momentum lost by shorter waves is imparted to longer waves. TAIRA and NAGATA (1968) observed that on a sloping beach in a wave-tank, capillary waves were generated in the process of breaking of a gravity wave train. If we assume that momentum lost by breaking of waves with a certain frequency still remains to be momentum of waves with another frequencies, the observed wave momentum flux shows that only a 10~20 % of the momentum imparted from air to sea is sufficient to develop wind-waves because viscous damping has little effects on longer waves which contain the largest part of the energy in a wave field.

In the wave generation theory established by Phillips, Miles and others, growth rate of spectral density is described by (cf. SNYDER and COX 1966)

$$\frac{dF(\sigma)}{dt}=\alpha+\beta F(\sigma) \qquad (6)$$

The first term α is due to the 'resonance' mechanism suggested by Phillips and it represents the initial stage of development. The second term $\beta F(\sigma)$ is due to the 'shear instability' mechanism proposed by Miles and it shows the main stage of development.

SNYDER and COX (1966) estimated α and β from observed growth rates of spectral density

* Here we assume that all wave trains are traveling in the same direction as the wind. DOBSON (1971) has estimated the error due to the angular spreadings of waves proportional to $\cos^2\theta$ where θ is the angle between wind and wave travel directions. He found that these estimates were reduced by 15 %.

for a particular wave component and suggested an empirical relation for β of the form

$$\beta = s\{\boldsymbol{k}\cdot\boldsymbol{W} - \sigma(\boldsymbol{k})\} \qquad (7)$$

where s is the ratio of the density of air to that of sea water, $\boldsymbol{k}$ propagation vector of the waves, $\sigma(\boldsymbol{k})$ corresponding angular frequency, and $\boldsymbol{W}$ mean wind velocity measured at the height of one wave length above the sea surface. Recent observational results by BARNETT and WILKERSON (1967), and IWATA and TANAKA (1970) agree with the relation.

Though the exponential growth with time is based on Miles's theory, the relation (7) gives a growth rate about ten times as large as that predicted by Miles's theory (cf. SNYDER and COX 1966, and BARNETT 1968). Moreover the wave momentum flux estimated by Equation (5) exceeds the momentum flux in the air as discussed below.

In the main stage of development, the exponential growth rate is much larger than the initial growth rate proportional to time. The increase of spectral density is approximated by the relation

$$\frac{dF(\sigma)}{dt} = \beta F(\sigma) = s\{\boldsymbol{k}\cdot\boldsymbol{W} - \sigma(\boldsymbol{k})\}F(\sigma) \qquad (8)$$

Taking a spectral density $F(\sigma)$ saturated to a frequency σ_e

$$F(\sigma) = \begin{cases} \varepsilon g^2\sigma^{-5} & \text{for} \quad \sigma \geqq \sigma_e \\ 0 & \text{for} \quad \sigma < \sigma_e \end{cases} \qquad (9)$$

and substituting (8) and (9) into (5), we have (cf. SNYDER and COX 1966)

$$\tau_w = \rho g s \varepsilon \int_{\sigma_e}^{\infty} \left(1 - \frac{g}{\sigma W}\right)\frac{W}{\sigma^2}\, d\sigma \qquad (10)$$

Here we assumed that all waves were propagating in the same direction as the wind and that the dispersion relation $\sigma^2 = gk$ for deep water was valid. Note that momentum flux imparted to waves with frequencies σ lower than σ_e cannot remain to be momentum of the waves and that the increment of energy $\Delta F(\sigma) = \beta F(\sigma)\cdot\Delta t$ is assumed to be transferred instantaneously to water motions of another kinds such as currents and turbulent motions. Consider a 'fully developed' state where the waves of which phase velocity is equal to the wind speed have grown up to compose an equilibrium spectrum. Putting $\sigma_e = g/W$ we find

$$\tau_w = \frac{1}{2}\varepsilon s \rho W^2 \qquad (11)$$

The wind stress is expressed by

$$\tau_a = \rho_a c_d W^2 \qquad (12)$$

The ratio of the wave momentum flux to the wind stress is

$$\tau_w/\tau_a = \varepsilon/2\, c_d \qquad (13)$$

Substituting empirical values of $\varepsilon = 1.17\times10^{-2}$ and $c_d = 1.3\times10^{-3}$, we find the ratio to be $\tau_w = 5.0\,\tau_a$ which can not be physically accepted.

When Miles's theory turns out to be unable to account for the actual growth rate, LONGUET-HIGGINS (1969) has proposed a new mechanism for the generation of sea waves. The 'virtual tangential stress' $2\rho\nu(ak)^2\sigma$ of shorter waves is transferred to the momentum of longer waves which propagate faster than the shorter waves, where ν is the kinematic molecular viscosity. After the shorter waves have decayed mainly on the crests of longer waves, the shorter waves are regenerated effectively by the wind before the successive crest of the longer waves comes. The momentum from the wind is essentially used to develop only the longer waves. The amplitudes of the longer waves increase in proportion to time as a result of the process:

$$a \sim \frac{\tau_a}{\rho g}\sigma t \qquad (14)$$

Since a spectral density is proportional to squares of wave amplitudes (cf. KINSMAN 1965, Chapt. 12), the spectral density is expected to

increase in proportion to the square of the duration according to this theory. However, this mechanism has not been verified by observations.

3. The Experiment

A series of field observations was carried out in the Lake Kasumigaura located about 70 km northeast of Tokyo (Figure 1) as a part of group studies on the evaporation from the lake in December, 1969. A capacitance wave gauge, with a sensing element of 1.2 mm Teflon-coated wire, was set at the end of a pier where the water depth was 80.0 cm. The pier was projecting about twelve meters northward from the lake shore. The output signals were recorded on a magnetic tape in the instrumentation shack about fifty meters from the shore.

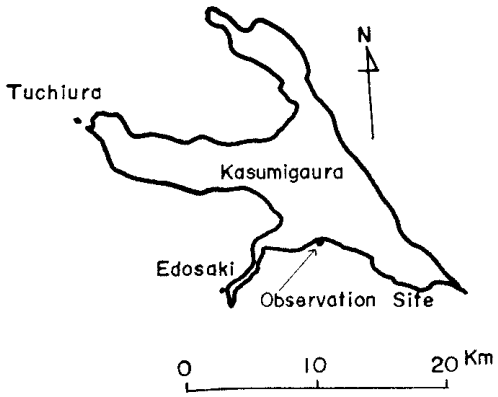

Fig. 1. Map of the observation site.

The hourly wind condition on December 13 is shown in Figure 2. The wind was measured with an anemometer of vane type mounted on the top of a pole 220 cm high above the water level. A sudden increase in the wind speed occurred at 11 a.m. is the most striking. The seasonal wind in winter had begun to blow. Theretofore, an unsteady wind was blowing with a speed less than 3 m/sec for about ten hours. After the step-wise increase the wind was blowing from a constant direction of northeast. Precise wind data were collected with an array of ten cup-anemometers (set at heights of 0.2 m, 0.5 m, 0.8 m, 1.1 m, 1.4 m, 3.0 m,

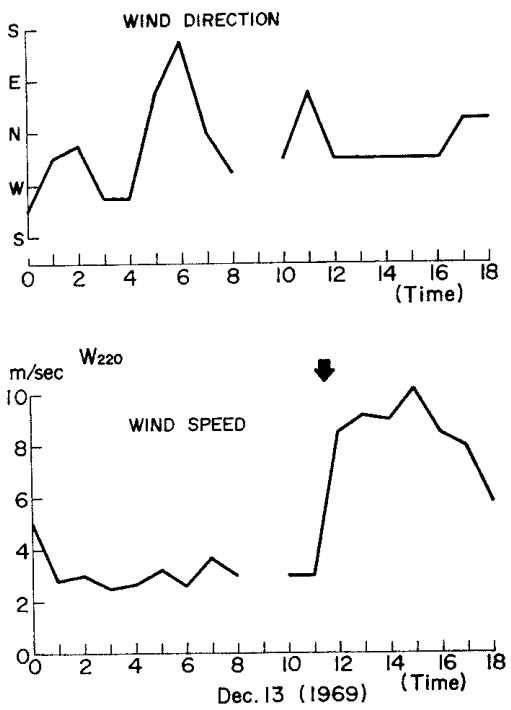

Fig. 2. Records of wind direction and speed at 220 cm height above the water level. Data for 8:00–10:00 were not available due to interruption of electricity.

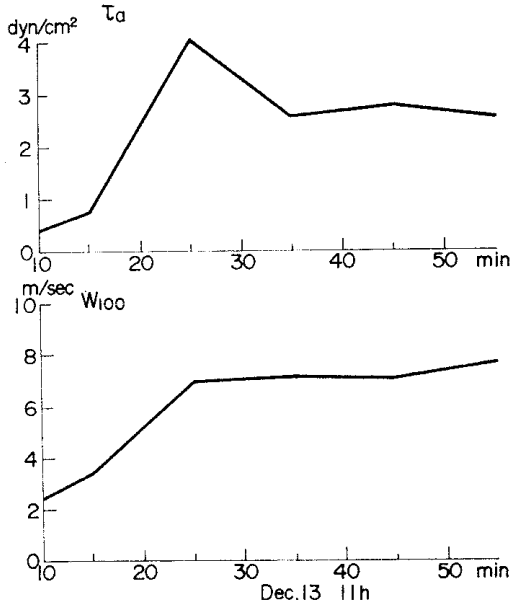

Fig. 3. Wind stress averaged over ten minutes estimated from the wind profile observed at ten heights from 0.2~14.0 m above the water level (upper) and the wind speed at 100 cm height (lower).

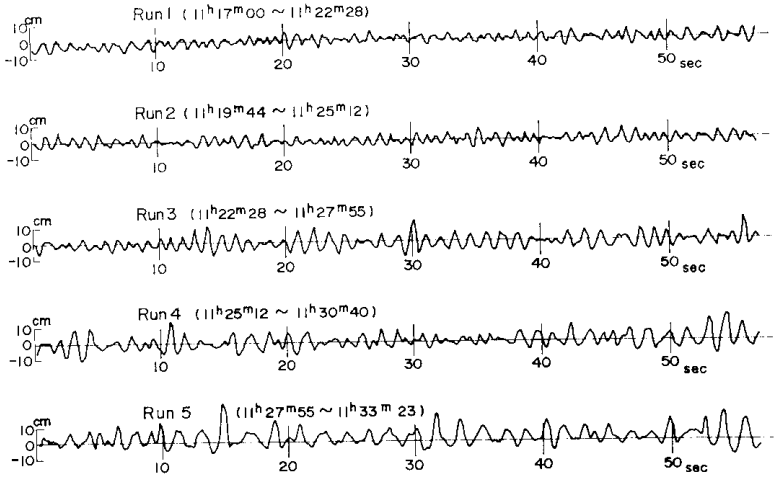

Fig. 4a. Examples of wave recorcs for Runs 1~5.

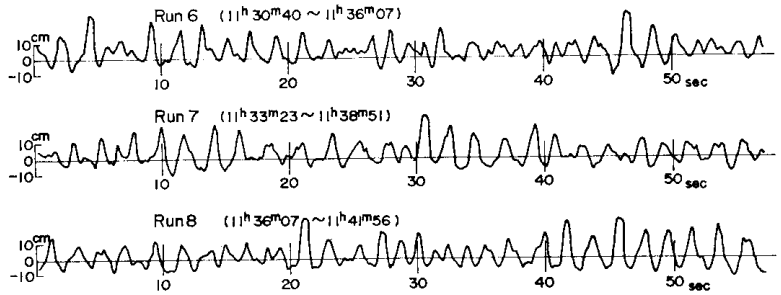

Fig. 4b. Examples of wave records for Runs 6~8.

5.0 m, 7.0 m, 10.0 m and 14.0 m above the water level).* The wind speeds at 1.0 m height (interpolated values) averaged over ten minutes are plotted in the lower portion of Figure 3. The sudden increase of wind speed occurred at 11:20. The wind stress was estimated by the wind profile method and the results are shown in the upper portion of Figure 3.

Recording of wave-height signals was started at 11:17 a.m. On playback these signals were digitized. Sampling time interval was 0.16 sec and total number of data was 9,216 (about 24.6 minutes). These digital data were divided into eight subgroups. Since each run needed 2,048 data to obtain sufficient stability of spectral estimates, overlapped time series were analyzed. The records of the first 60 sec for each run are plotted in Figures 4a and 4b, and the observational period for each run is noted to the records. The figures reveal the rapid development of wind-waves caused by the strong seasonal wind.

The wind stress plotted in Figure 3 may be somewhat larger than that expected for these wind speeds.* In Figures 4a and 4b, we took the mean value of Run 1 as the zero-level for each run. We notice the increase of water

* These wind data were collected and analyzed by a research group of the Japan Meterological Agency.

* The wind stress was also estimated by the eddy correlation method (MITSUTA, HANAFUSA, MAITANI and FUJITANI 1970). Their results show the wind stress exerting in the period from 11:36 to 12:29 to be 1.51 dyn/cm^2. The mean stress estimated by the profile method in the period is 2.01 dyn/cm^2 which is about 130 % as large as the former.

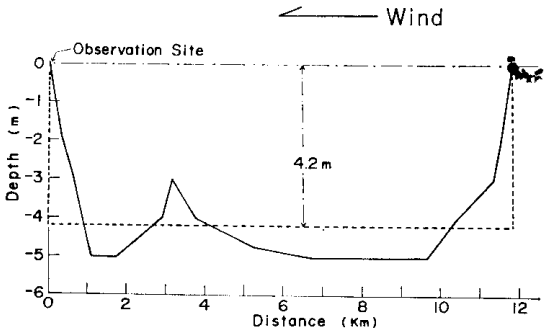

Fig. 5. The cross section of the bottom topography of the lake in the upwind direction of the observation site.

level which must have been caused by the wind set-up. The difference of the mean water level between the first and the last run was 6.04 cm. The distance from the up-wind shore to the observational site was about 12 km as shown in Figure 5. If we assume that the lake is a rectangular water with the depth of $h=4.2$ m and the length of 12 km and that the state is stationary, we can estimate the wind stress exerting on the water surface by the relation $\tau_0=\rho gih$ where i is the surface slope. The relation gives $\tau_0=4.1$ dyn/cm^2, which is in acccord with the maximum wind stress in the observational period. The above assumed rectangular basin is, however, an artificial one. If one consider another basin from Tsuchiura to the observational site, the fetch is about 20 km. The relation gives $\tau_0=2.46$ dyn/cm^2 and it accords with the mean stress in the period.

4. Analysis of the wave records

(i) Significant waves

Significant waves were calculated for each observational run and the results are tabulated in Table 1. Hence each run took 327.68 sec (=0.16 sec×2048), the number of significant waves contained in Run 1 is 330 and that in Run 8 is 150 approximately. Phase velocity $C_{1/3}$, wave energy $E(=\rho gH^2{}_{1/3}/8.0$ erg/cm$^2)$, and wave momentum $M(=E/C_{1/3}$ dyn·sec/cm$^2)$ were calculated for these significant waves.

Wave momentum flux $\tau_w{}^*$ was estimated by Equation (3) which was replaced by a finite difference of the form

Table 1. Significant waves.

Run	$H_{1/3}$ (cm)	$T_{1/3}$ (sec)	$C_{1/3}$ (cm/sec)	E (erg/cm^2)	M (dyn·sec/cm^2)
1	9.10	0.99	154.5	10144	65.66
2	11.86	1.17	179.5	17230	95.99
3	13.74	1.26	190.5	23126	121.40
4	15.45	1.35	200.0	29241	146.21
5	19.75	1.55	217.4	47783	219.79
6	22.79	1.77	232.2	63625	274.00
7	23.96	1.89	238.0	70325	295.48
8	25.19	2.07	244.4	77731	318.05

Table 2. Wind stress τ_a and wave momentum flux estimated by two ways: τ^w... by significant waves.

Run	τ_a (dyn/cm^2)	τ^w (dyn/cm^2)	τ^w/τ^a (%)	τ_a (dyn/cm^2)	τ^w/τ_a (%)
2-1	2.30	0.110	5	0.137	6
3-2	3.25	0.115	3	0.118	4
4-3	3.91	0.111	3	0.157	4
5-4	3.60	0.355	10	0.358	10
6-5	3.25	0.232	7	0.261	8
7-6	2.75	0.088	3	0.176	6
8-7	2.55	0.088	3	0.215	8

$$\tau_w{}^*=\frac{2}{C_{N+1}+C_N}\cdot\frac{E_{N+1}-E_N}{\Delta t}-\frac{2(E_{N+1}+E_N)}{(C_{N+1}+C_N)^2}\cdot\frac{C_{N+1}-C_N}{\Delta t}$$

where $\Delta t(=163.84$ sec) is the elapsed time and C_N is the phase velocity of significant waves for N-th run. Calculated wave momentum fluxes are tabulated in the second column of Table 2. The wind stress in the observational period was read out from the upper graph of Figure 3. The ratio of the wave momentum flux to the wind stress $\tau_w{}^*/\tau_a$ was estimated to be (in the third column of Table 2)

$$\tau_w{}^*=(0.03\sim0.10)\tau_a$$

The mean value of the ratio is $\tau_w{}^*=0.051\,\tau_a$ which is smaller than $0.2\,\tau_a$ estimated by STEWART (1961). The observed value is near to $0.1\,\tau_a$ by STARR (1947) or $(0.06\sim0.07)\,\tau_a$ by KORVIN-KROUKOVSKY (1965).

(ii) Spectral analysis

Power spectra were computed for each run by using a program based on the algorithm of the Fast Fourier Transform (cf. TAIRA 1971b). The spectral density $\Phi(f)$ is defined so that

$$\overline{\zeta}^2=\int_{-\infty}^{\infty}\Phi(f)df$$

where $\overline{\zeta}^2$ is the covariance. An equilibrium spectrum $F(\sigma)=\varepsilon g^2\sigma^{-5}$ ($\varepsilon=1.17\times10^{-2}$, suggested by PHILLIPS 1966) for a spectral density $F(\sigma)$ defined by $\overline{\zeta}^2=\int_0^{\infty}F(\sigma)\,d\sigma$ is described by $\Phi(f)=3.61f^{-5}$. Figure 6 shows the computed power spectra. The observed values are well expressed by the straight line denoting the equilibrium spectrum.

The wave momentum flux τ_w was estimated by (5) replacing the integration by a sum:

$$\tau_w=2\rho g\sum_{i=0}^{m}\frac{\Delta\Phi(f_i)}{C(f_i)}\cdot\frac{\Delta f}{\Delta t}$$

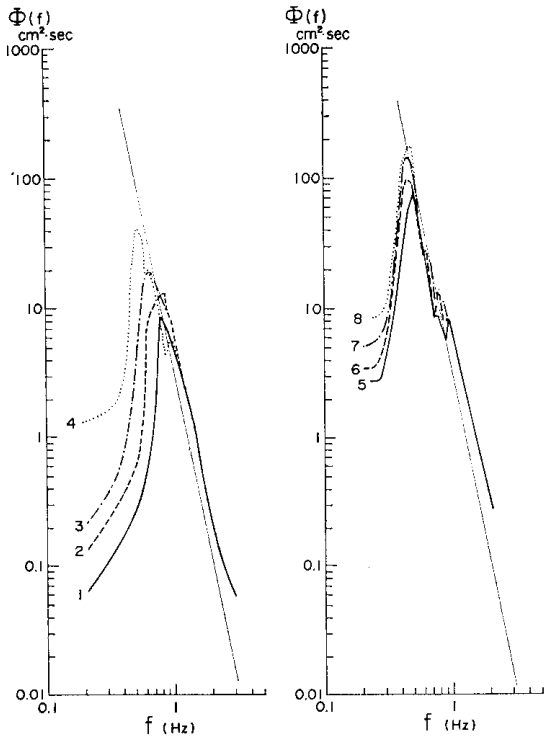

Fig. 6. Power spectra for wave records of each run.

where $\Delta f=0.0305$ Hz is the frequency resolution in our analysis and $\Delta\Phi(f_i)$ denotes the difference of spectral densities observed in the two successive runs and it is plotted in Figure 10. The wave momentum fluxes are tabulated in the fourth column of Table 2. The ratio to the wind stress is found to be $\tau_w=(0.04\sim0.10)\,\tau_a$. The mean value is $\tau_w=0.066\,\tau_a$ which is in good accord with that estimated by the significant waves.

(iii) Comparison with the observation of SNYDER and COX

Spectral growth rate of a particular wave component was compared with the observational result by SNYDER and COX (1966) which is represented by Equation (7). Spectral densities for the frequency of 0.4578 Hz were selected because these waves showed the most rapid growth in our observations and they composed the main peak of the spectrum for Run 8. The

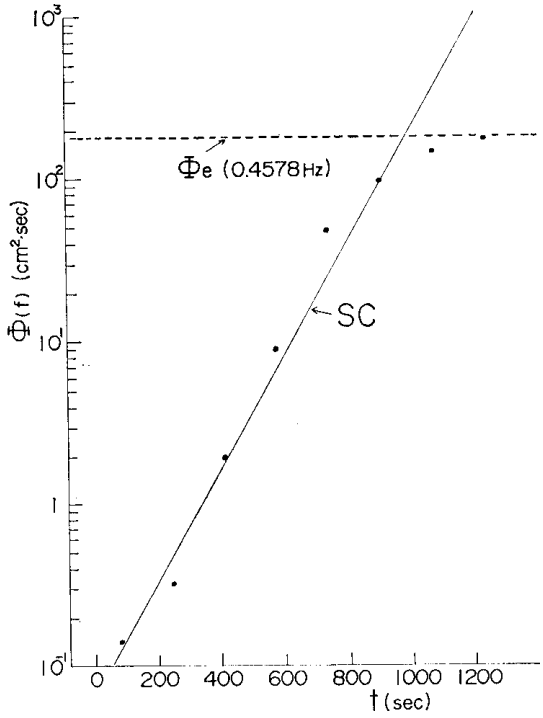

Fig. 7. The growth of power spectral densities for wave component of $f=0.4578$ Hz versus duration. The curve marked SC represents the empirical suggestion of SYNDER and COX (1966). Exponential growth-rate analysis.

wave number corresponding to the frequency is $K=0.01158\,\mathrm{cm}^{-1}$ in the water of 80.0 cm depth where the measurements were carried out. The wind speeds at the heights of 5.0 m and 7.0 m were averaged and the mean wind speed was $W=820$ cm/sec. Putting these numerical values into (7) we have

$$\beta=s(KW-\sigma)\doteqdot 0.0079\ \mathrm{sec}^{-1}$$

The spectral density $\Phi(f)$ is predicted to be

$$\ln\Phi(f)=\beta t+c'=\beta t'$$

In Figure 7, the observed spectral densities are plotted on a log-scale and the duration t is plotted on a linear scale so that the above relation is expressed by a straight line. Observed spectral densities are well expressed by this straight line until they approach to the equilibrium value for the frequency. As previously reported (cf. SNYDER and COX 1966), the observed growth rate diminishes for spectral densities greater than about 30 % of the equilibrium value.

For the case of Run 8 the wave momentum flux was estimated by Equation (10). Taking the peak frequency of $\sigma_c=2.876\,\mathrm{sec}^{-1}$, we found $\tau_w=3.01\,\mathrm{dyn/cm}^2$ which exceeded the wind

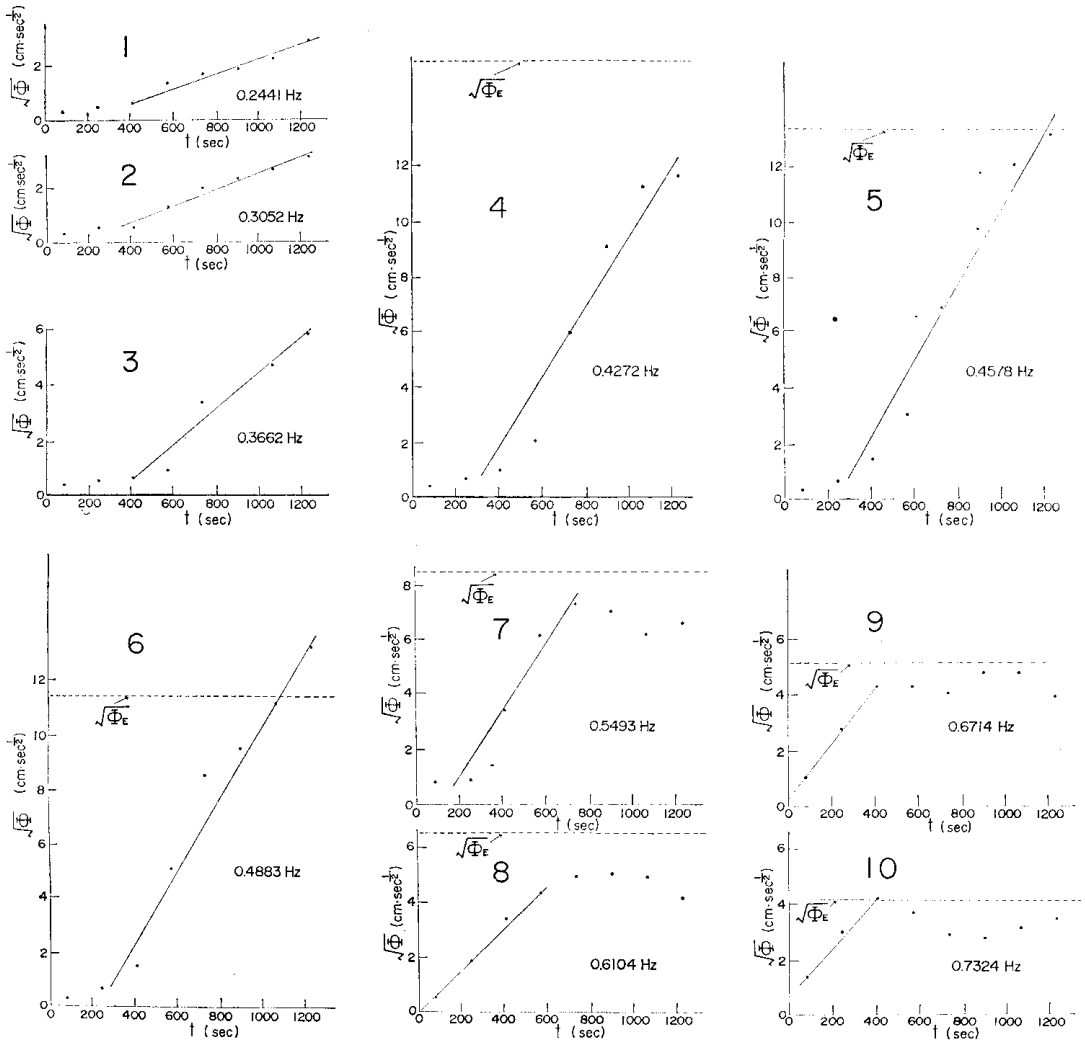

Fig. 8. The square root of spectral density versus duration. The quadratic growth-rate analysis.

stress 2.55 dyn/cm² in the observational period.

(iv) Comparison with the theory of Longuet-Higgins

LONGUET-HIGGINS (1969) has proposed a new generation mechanism: the wave amplitude increases in proportion to the duration as described by Equation (14). According to this theory, the spectral density is described by

$$\Phi(f)=\gamma^2 t'^2 \qquad (15)$$

In Figure 8, the square roots of the observed spectral densities are plotted against the duration so that the relation (15) is expressed by a straight line. The observed spectral densities satisfy the relation (15) very well. It may seem to be curious that the same data can be expressed well both by the two curves: by the exponential curve $exp\,(\beta t')$ and by the quadratic curve $\gamma^2 t'^2$. Compare Figure 7 with the graph 5 of Figure 8 for the frequency 0.4578 Hz. In Figure 7 the last two spectral densities observed in Run 7 and Run 8 which are 81.1 % and 96.5 % of the equilibrium value for the frequency, respectively, are far smaller than the values predicted by the exponential growth curve. On the other hand, these two spectral densities agree well with the quadratic curve as shown by the graph 5 of Figure 8.

Figure 8 shows the comparison of observed spectral densities with the quadratic growth curves for frequencies at which spectral densities have grown up to their equilibrium values (graph 5~10). Graphs 1~4 of the figure, however, show the spectral densities which composed the 'leading edge' of the spectrum of Run 8. At these frequencies of wider range, the quadratic growth curves predict well the observed values which sometimes exceeded the equilibrium values.

The term γ defined by Equation (15) was determined graphically for the rapid growth of each graph in Figure 8. The values are plotted against the wave frequency in Figure 9. Observed spectral densities are generally described by

$$\Phi(f)=\{r(f)\,(t-t_f)\}^2$$

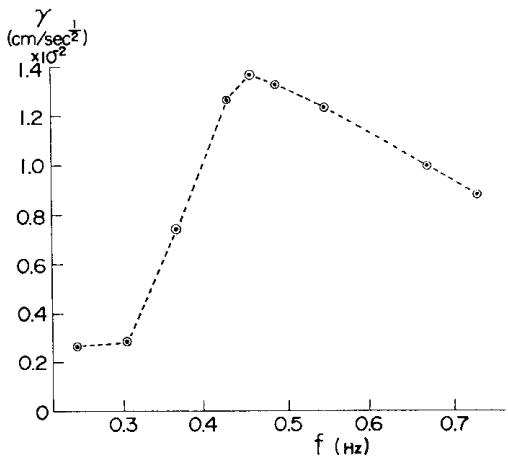

Fig. 9. The empirical coefficient $\gamma(f)$ in $\Phi(f)=\{r(f)\cdot(t-t_f)\}$ determined from the graphs in Figure 8.

where t_f is the start time of the rapid growth for the frequency and it becomes larger for lower frequencies. The quadratic growth rate $\gamma(f)$ shows a maximum at a frequency where observed spectral densities had attained to the equilibrium values for the last observational run.

The tendency of decrease of $\gamma(f)$ at lower frequencies may be explained, according to the theory of LONGUET-HIGGINS, by the fact that the wave steepness is too small to obtain the virtual tangential stress of shorter waves. We can not derive a precise frequency-dependence of the growth rates predicted by the theory because it is derived originally for a characteristic wave train for a wave field. As described in the later sections, another mechanism is suggested to be responsible for the rapid growth of wind-waves, the theory is not investigated further in this paper.

5. The 'overshoot effect' of spectral densities

BARNETT and SUTHERLAND (1968) have studied the phenomenon which was termed the 'overshoot effect' by BARNETT and WILKERSON (1967). In the rapid stage of development, spectral densities of a particular Fourier component grow as the fetch increases until they attain to the maximum which is much larger than the equilibrium value for the frequency. This is the 'overshoot effect'. After having

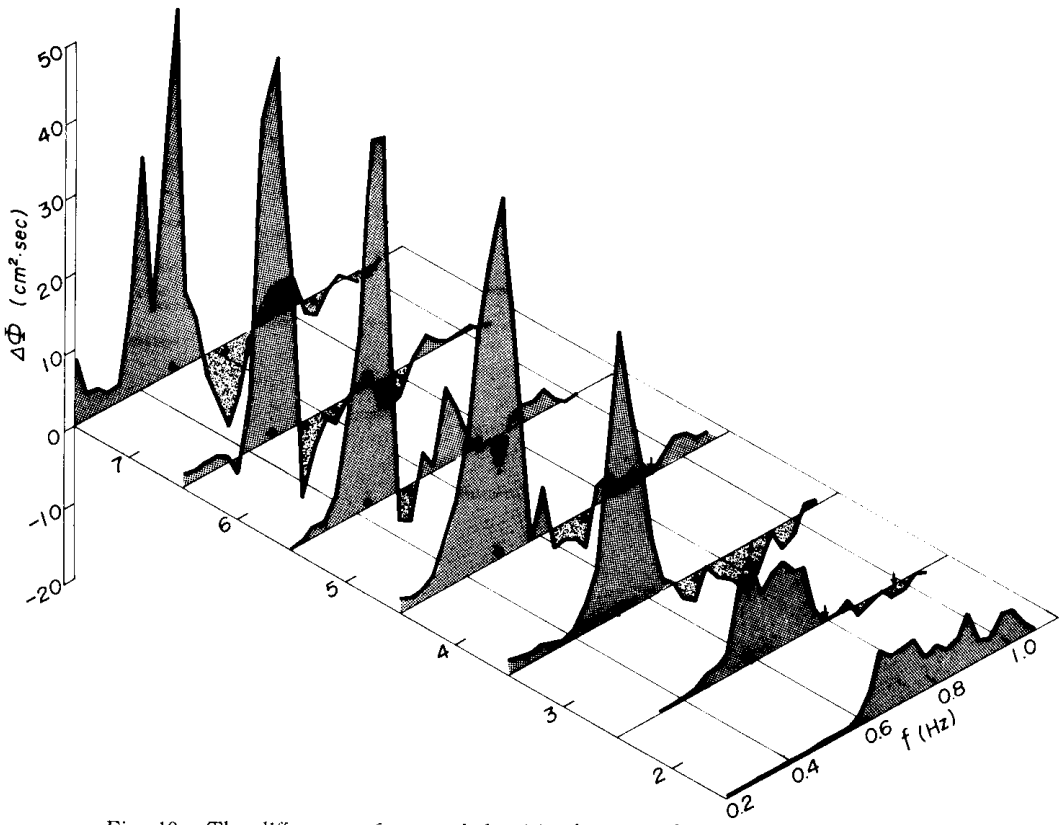

Fig. 10. The difference of spectral densities between the two successive runs versus the wave frequency.

attained to the maximum, the spectral densities decrease as the fetch increases and they show a minimum which is about 50 % of the maximum. BARNETT and SUTHERLAND termed this decrease as the 'undershoot effect'. After the undershoot the spectral densities increase again and several slowly-decaying oscillations are observed. BARNETT and SUTHERLAND (1968), and MITSUYASU (1969) studied some characteristics of the overshoot-undershoot effects but they could not establish the mechanism responsible for these phenomena.

We examined the frequency-relations of the overshoot-undershoot effects among the wave components. Figure 10 shows the difference of the spectral densities between the two successive observational runs plotted as a function of both the duration and the wave frequency. For given duration, the largest positive values at the lowest frequencies show that the spectral densities are growing most rapidly at these frequencies. They eventually exceed the equilibrium values and the overshoot effect will occure. The negative values at higher frequencies indicate that the undershoot effects are taking place, and the positive values at higher frequencies show that the spectral densities are growing again after the undershoot.

In Figure 10, the most striking fact is that the positive values indicating the increasing spectral densities are distributed over discrete frequencies for a given duration. These characteristics are emphasized for the longer duration. We could not find any negative values for the earliest runs. Since the largest increase of spectral densities is achieved for a limited frequency band, the wave generation theories by PHILLIPS or MILES are hardly expected to be applied. These phenomena have been observed in the observations at a marine tower.*

* The data for TAIRA (1971a) showed these phenomena and they will be discussed elsewhere.

Table 3. Three characteristic waves for the observed spectral growth.

Run	f_1 (Hz)	f_3 (Hz)	f_2 (Hz)	$\frac{f_1+f_2}{2f_3}$	k_1 (cm^{-1})	k_3 (cm^{-1})	k_2 (cm^{-1})	$\frac{k_1+k_2}{2k_3}$	$-\frac{(\Delta\Phi(f_2)+\Delta\Phi(f_3))}{\Delta\Phi(f_1)}$
3-2	0.580	0.793	0.977	0.982	0.0135	0.0254	0.0384	1.022	15%
					0.0159	0.0261	0.0386	1.044	
4-3	0.519	0.732	0.885	0.959	0.0108	0.0216	0.0316	0.981	19%
					0.0136	0.0228	0.0319	0.998	
5-4	0.488	0.732	0.916	0.959	0.0096	0.0216	0.0338	1.005	12%
					0.0126	0.0228	0.0341	0.974	
6-5	0.427	0.549	0.732	1.056	0.0074	0.0122	0.0216	1.188	11%
					0.0106	0.0147	0.0228	1.136	
7-6	0.458	0.549	0.641	1.001	0.0085	0.0122	0.0165	1.022	26%
					0.0116	0.0147	0.0184	1.020	
8-7	0.488	0.641	0.885	1.071	0.0096	0.0165	0.0316	1.248	31%
					0.0126	0.0184	0.0319	1.209	

To characterize the discreteness of the frequency distribution of positive or negative values, we chose three characteristic frequencies: f_1 the central frequency of the lowest positive values, f_3 the central frequency of the lowest negative values, and f_2 the central frequency of the negative values next to those at f_3. These frequencies for each duration are noted by arrows in Figure 10 and they are also tabulated in Table 3. We find that the next relation is satisfied by the frequencies:

$$f_1+f_2=2f_3 \qquad (16)$$

In the fourth column of Table 3, the ratio $(f_1+f_2)/2f_3$ is shown and it varies from 0.959 to 1.071. We estimated the spectral densities by averaging the squares of Fourier coefficients over a frequency band Δf. When the relation (16) is strictly satisfied in reality, the observed ratio $(f_1+f_2)/2f_3$ may fluctuate from $(1-\Delta f/f_3)/(1+\Delta f/f_3)$ to $(1+\Delta f/f_3)/(1-\Delta f/f_3)$. By taking the numerical values $\Delta f=0.0305$ Hz of our analysis and $f_3=0.6$ Hz, for instance, we find this range to be 0.905-1.105. The observed ratio is distributed in this range.

The wave numbers related with the frequencies by $(2\pi f)^2=gk\tanh kh$ were calculated and tabulated in Table 3. Of the pairs of wave numbers, the value in the upper lines show those for $h=420$ cm which is the mean depth of the lake (Figure 5). The lower values represent the wave numbers for $h=80$ cm which is the depth of the observational site. The calculated wave numbers satisfy approximately the relation

$$k_1+k_2=2k_3 \qquad (17)$$

The ratio $(k_1+k_2)/2k_3$ was calculated and tabulated in the eighth column.

It is interesting to examine whether the energy lost at the two negative regions (centered at f_3 and f_2) is sufficient to feed the energy of the positive region centered at f_1. In the last column of Table 3, the ratio of the decreased energy to the increased energy is tabulated. Since the ratio varies from 11 % to 31 %, the energy exchange among the three regions is insufficient to explain the growth of the observed spectral densities at the lower frequencies.

6. Discussion

The relations (16) and (17) are the resonance conditions for wave-wave interactions among three wave components, which are special cases of the interactions among four wave components. PHILLIPS (1960) and LONGUET-HIGGINS (1962) have studied theoretically these interactions. According to LONGUET-HIGGINS, when the three wave trains satisfy the resonance conditions:

$$\sigma_1+\sigma_2=2\sigma_3 \qquad (18)$$

and

$$\boldsymbol{k}_1+\boldsymbol{k}_2=2\,\boldsymbol{k}_3 \qquad (19)$$

the amplitude of the wave component ($\boldsymbol{k}_1$, σ_1) increases with time as described by

$$a_1=(a_2k_2)(a_3k_3)^2\frac{1}{2}g\iota\,\sigma_3^{-1}\hat{f}(\xi) \qquad (20)$$

provided that the wave steepness of the waves a_1k_1 is far smaller than both a_2k_2 and a_3k_3. The parameter ξ in (20) denotes the frequency ratio:

$$\xi=(\sigma_2-\sigma_3)/\sigma_3 \qquad (21)$$

The function $\hat{f}(\xi)$ is expressed by

$$\hat{f}(\xi)=\frac{\left(1+\frac{1}{2}\xi^2\right)^2(1-4\xi^2)}{(1+\xi)^3}\times\left\{1+\frac{4\xi}{\xi-(6+\xi^2)^{1/2}}\right\} \qquad (22)$$

The angle θ of intersection of the primary waves ($\boldsymbol{k}_2$ and $\boldsymbol{k}_3$) is represented by the relation

$$\cos^2\frac{1}{2}\theta=\frac{(1+2\xi)(2+\xi^2)}{2(1+\xi)^2} \qquad (23)$$

For a particular case where $\theta=\pi/2$ and $\xi<0$, LONGUET-HIGGINS and SMITH (1966) and MCGOLDRICK, PHILLIPS, HUANG and HODGSON (1966) carried out experiments in wave-tanks to confirm the wave-wave interactions and succeeded to obtain experimental results close to the predicted values. In their experiments, the energy of the primary waves was transferred to that of the higher-frequency waves because ξ is negative. In the experiments by MCGOLDRICK, PHILLIPS, HUANG and HODGSON, the waves produced in the process of interactions grow with time as predicted by (20) and attain to wave-steepness of $a_1k_1=0.0474$ in a distance only twenty times as long as the wave length. The wave-steepness is about 53 % and 56 % of that of primary waves, a_3k_3 and a_2k_2, respectively.

The amplitudes of the wave components grow linearly with time as a result of the wave-wave interactions (Equation 20) and the power spectrum must be a function of ι^2. Since the spectral growth in our experiment is also well described by a function of ι^2, it is suggested that these wave-wave interactions might be responsible for the development of wind-waves.

In the process of development of wind-waves, the energy must be transferred from higher-frequency components to lower-frequency components because the spectral densities of the former will attain to the equilibrium values before those of the latter. In such wave-wave interactions, the frequency ratio ξ defined by Equation (21) is positive. The values of $\hat{f}(\xi)$ and θ are calculated for positive values of ξ by the use of Equations (22) and (23) and they are plotted in Figure 11. The function $\hat{f}(\xi)$ decreases monotonously as ξ becomes larger and it vanishes when $\zeta=\frac{1}{2}$ (see LONGUET-HIGGINS, 1962). The angle θ of intersection of the primary waves is limited in a narrow band less than 11.9° as shown in the upper portion of Figure

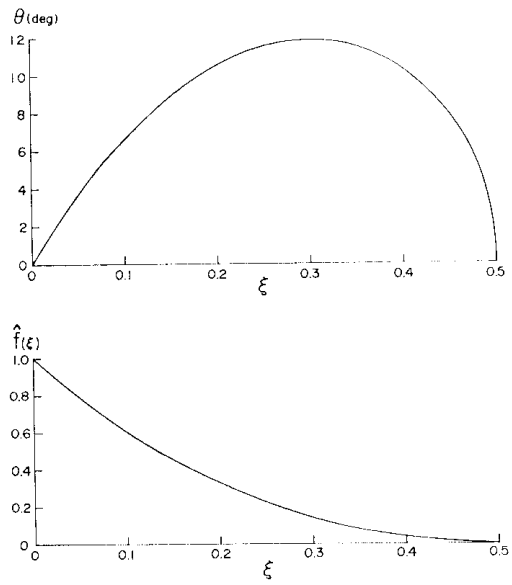

Fig. 11. The intersection angle θ between the primary waves for wave-wave interactions among three wave trains (upper) and coupling coefficieents $f(\xi)$ versus the positive values of ξ (lower) according to LONGUET-HIGGINS (1962).

11. The waves propagating in almost the same direction can resonate. The fact well explains why the observed resonance condition can be represented by a scaler relation of Equation (17) which is equivalent to the vectorial relation of Equation (19) only when the three waves are propagating in the same direction.

BENNEY (1962) studied theoretically the energy exchange among the resonant waves with wave steepness of nearly the same order and he found that no stable equilibrium amplitudes could be expected. The phenomenon seems to be able to explain the ceaseless oscillations of spectral densities in the overshoot-undershoot stage of actual wind-waves.

BENNEY showed the relations among the amplitudes of three interacting waves:

$$\left.\begin{aligned} &\frac{a_1^2}{\sigma_1}-\frac{a_2^2}{\sigma_2}=\text{constant} \\ &2\frac{a_1^2}{\sigma_1}+\frac{a_3^2}{\sigma_3}=\text{constant} \end{aligned}\right\} \qquad (24)$$

These relations show that a_1 and a_2 increase when a_3 decreases. In our analysis described in the previous section, both a_2 and a_3 are the center frequencies of bands where the spectral densities are decreasing. The relations of (24) represent the conservation of the total energy as

$$\begin{aligned} a_1^2+a_2^2+a_3^2 &= a_1^2(\sigma_1+\sigma_2-2\sigma_3)/\sigma_1+\text{constant} \\ &= \text{constant} \end{aligned}$$

and also represent the conservation of the total momentum (see, PHILLIPS, 1966). Apparently the energy of the actual wind-waves is not conserved. It must be increasing due to the supply from the winds. Over the equilibrium range, there must be many sets of interactions (generally among four wave trains) and the shape of the spectrum is expected to become an universal one as a result of them. Since the energy exchange is not effective for a larger value of ξ, a cascade of wave-wave interactions is considered to be transferring the energy from higher-frequency components to lower-frequency components. Our analysis showed that the rate of energy exchange was so effective that we could not detect a set of interacting wave trains in the earliest runs of which time interval was about 300 times as long as these wave periods.

As discussed above, the wave-wave interactions are suggested to be a mechanism most responsible for both the rapid growth stage and the overshoot-undershoot stage of wind-waves. Theoretical results for the interactions are desired to be applied to the process of observed spectral growth. Theories are derived for interactions among long-crested wave trains as shown by Equation (20). On the other hand, observational results are described by a continuous spectrum. For applying the equation to the observational results, we need further considerations: (i) how we determine the amplitude of a long-crested wave train from the observed spectral density, and (ii) what is the physical meaning of the equilibrium spectrum that is expected to be realized through the interactions. Obviously these questions have not been solved yet.

HASSELMANN (1962, 1963) studied theoretically the energy transfer in a gravity-wave spectrum. He showed that in a continuous spectrum the energy changed linearly with time and that the energy flux favoured equidistribution of energy and vanished in the limiting case of a white, isotropic spectrum. He applied his theory to the swell attenuation in the Pacific Ocean radiated from storms at South of New Zealand to Alaska and he suggested that the features of the observed decay were consistent with the computed energy transfer (SNODGRASS, GROVES. HASSELMANN, MILLER, MUNK and POWERS 1966).

BARNETT (1968) parameterized Hasselmann's results which originally involved cubic integrations into a simple form. He applied it to his wave prediction scheme. The wave-wave interactions played a little role in the developing stage, because BARNETT adopted the exponential growth rate similar to (7) and the dampling factor which eventually reduced the computed spectrum into an equilibrium spectrum. INOUE (1967) hindcasted the same situation using a scheme without the terms of wave-wave interactions and obtained almost the same results

as BARNETT (1968). MITSUYASU (1968) applied the simple form of Hasselmann's results parameterized by BARNETT to a decay process of wind-waves generated in a wind-flume and he showed that the measured rate of energy transfer was very close to the predicted one. On the other hand, BARNETT and SUTHERLAND (1968) failed to explain the overshoot-undershoot effects which occurred under the action of the wind by applying the parameterized form.

As reviewed above, Hasselmann's theoretical results on the energy exchange in a continuous spectrum can be successfully applied to wave decay process without the action of the wind. This process is considered to be approximated sufficiently by a process of "whitening" of the energy spectrum, that is to say, a process of equidistribution of energy over a wide frequency range from almost D.C. (oceanic currents) to very high frequencies (waves or turbulence) where the energy is transformed effectively into heat under the action of viscosity. In the process of wave growth the equilibrium shape of the energy spectra is different far from that of a white spectrum. The observed spectra for developing wind-waves are subject to the well-known 'law of σ^{-5}', to which our observational results are also subject as described before.

Here we propose a hypothesis that the wave steepness of each wave train which composes the equilibrium spectrum is equalized. Though the hypothesis is suggested by the fact that the magnitude of wave steepness determines the rate of energy exchange in Equation (20), the wave steepness represents surface slope due to wave motion and it is generally a scale of intensity of nonlinearity in the theory for water waves. It seems to be very natural to assume that this parameter is equalized in the process of nonlinear interactions. Some model studies based on the hypothesis will be made in Part 2.

Acknowledgments

I wish to express my thanks to Prof. Y. OGURA and Mr. A. TAKEDA for their encouragements. My sincerest thanks are also to Profs. K. YOSHIDA, K. KAJIURA and Y. NAGATA for their kind advices. Thanks are due to Mr. K. ISHIKAWA, Mr. N. MISAWA and Mrs. J. ENDOH for their assistance and to all the members of the project for evaporation study represented by Prof. G. YAMAMOTO of Tohoku University.

References

BARNETT, T.P. and J.C. WILKERSON (1967): On the generation of ocean waves as inferred from airborne radar measurements of fetch-limited spectra. J. Marine Res. **25**, 292–328.

BARNETT, T.P. (1968): On the generation, dissipation, and prediction of ocean wind waves. J. Geophys. Res. **73**, 513–529.

BARNETT, T.P., and A.J. SUTHERLAND (1968): A note on an overshoot effect in wind-generated waves. J. Geophys. Res. **73**, 6879–1885.

BENNEY, D.J. (1962): Non-linear gravity wave interactions. J. Fluid Mech. **14**, 577–584.

DOBSON, F.W. (1971): Measurements of atmospheric pressure on wind-generated sea waves. J. Fluid Mech. **48**, 91–127.

HAMADA, T., A. SHIBAYAMA and H. KATO (1966): A note on the development of wind waves in an experiment. Port and Harbour Res. Inst. Ministry of Transport, Japan. Rept. no. **12**, 16–29.

HASSELMANN, K. (1962): On the non-linear energy transfer in a gravity wave spectrum. Part I: General theory. J. Fluid Mech. **12**, 481–500.

HASSELMANN, K. (1963): On the non-linear energy transfer in a gravity wave spectrum. Part II: Conservation theorems; wave particle analogy; irreversibility. J. Fluid Mech. **15**, 273–281.

INOUE, T. (1966): On the growth of the spectrum of a wind generated sea according to a modified Miles-Phillips Mechanism. Geophysical Sciences Lab. Rept. TR 66-6, School of Engineering Science, New York University.

IWATA, N. and T. TANAKA (1970): Spectral development of wind waves. Kokuritsu Bosai Kagakugijutsu Senta Kenkyu Hokoku, **4**, 1–21. (in Japanese)

KINSMAN, B. (1965): Wind waves. Prentice-Hall, Inc., Englewood Cliffs, N.J.

KORVIN-KROUKOVSKY, B.V. (1965): Balance of energies in the development of sea waves, Semi-empirial evaluation. Deut. Hydrograph. Z. **18**, 145–160.

LONGUET-HIGGINS, M.S. (1962): Resonant interactions between two trains of gravity waves. J. Fluid Mech. **12**, 321–332.

LONGUET-HIGGINS, M.S., and N.D. SMITH (1966): An experiment of third order resonant wave interactions. J. Fluid Mech. **25**, 417–435.

LONGUET-HIGGINS, M. S. (1969): A nonlinear mechanism for the generation of sea waves. Proc. Roy. Soc. A. **311**, 371-389.

MCGOLDRICK, L.F., O.M. PHILLIPS, N.E. HUANG, and T.H. HODGSON, (1966): Measurements of third-order resonant wave interactions. J. Fluid Mech. **25**, 193-217.

MITSUTA, Y., T. HANAFUSA, T. MAITANI and T. FUJITANI (1970): Turbulent fluxes over the Lake Kasumigaura. Special Contributions. Geophys. Inst. University of Kyoto. No. **10**, 75-84.

MITSUYASU, H. (1968): A note on the nonlinear energy transfer in the spectrum of wind generated waves. Rept. Res. Inst. for Applied Mechanics, Kyushu University. **XVI**, 251-264.

MITSUYASU, H. (1969): On the growth of the spectrum of wind-generated waves (II)-Note on the equilibrium spectrum and the Overshoot phenomena-. Rept. Res. Inst. for Applied Mechanics, Kyushu University. **XVII**, 235-248.

PHILLIPS, O.M. (1960): On the dynamics of unsteady gravity waves of finite amplitude. Part I. The elementary interactions. J. Fluid Mech. **9**, 193-217.

PHILLIPS, O.M. (1966): The dynamics of the upper ocean. Cambridge University Press.

SNODGRASS, F.E., G.W. GROVES, K.F. HASSELMANN, G.R. MILLER, W.H. MUNK and W.H. POWERS (1966): Propagation of ocean swell across the Pacific. Phil. Trans. Roy. Soc. London, A., **259**, 431-497.

SNYDER, R.L. and C.S. COX (1966): A field study of the wind generation of ocean waves. J. Marine Res., **24**, 141-178.

STARR, V.P. (1947): A momentum integral for surface waves in deep water. J. Marine Res. **VI**, 126-134.

STEWART, R.W. (1961): The wave drag of wind over water. J. Fluid Mech. **10**, 189-194.

SVERDRUP, H.U. and W.H. MUNK (1947): Wind, sea swell: theory of relations for forecasting. U.S. Navy Hydrogr. Office Pub. No. 601.

TAIRA, K. and Y. NAGATA (1968): Experimental study of wave reflection by a sloping beach. J. Oceanogr. Soc. Japan, **24**, 242-252.

TAIRA, K. (1971a): Measurements of momentum transfer from air to sea. Proc. Joint Oceanogr. Assembly (Tokyo, 1970): 202-204.

TAIRA, K. (1971b): Wave particle velocities measured with a Doppler current meter. J. Oceanogr. Soc. Japan. **27**, 218-232.

風波の成長についての野外研究

第1部 観 測 結 果

平 啓 介

要旨: 冬季の季節風の吹き出しによって，平均水深 420 cm，吹走距離 12 km の霞ケ浦で急速に成長した風波の観測結果について報告する。測定は湖岸から 10 m の水深 80 cm の地点で行なった。波の運動量フラックス，すなわち，波の運動量の時間微分を有義波とスペクトル密度とを用いて評価した。二つの方法はほぼ等しい値を与え，風から水に与えられる運動量フラックスの5～7%が波として残ることが明らかにされた。

一つの周波数成分のスペクトル密度の成長を，SNYDER and COX (1966)，その他が報告した指数関数的成長率と比較した。我々の測定値はこれらの値と一致している。従来の風波の成長理論で想定されているように，指数関数的成長率ですべての成分波が成長すると，風波の運動量フラックスは風からのフラックスを上まわることになり，観測値を説明できないだけでなく，物理学的にも不合理であることが示された。

吹送時間の経過に伴うスペクトル密度の増減を調べた。スペクトル密度の増加は，いくつかの周波数帯に限られていることがわかった。このことは BARNETT and SUTHERLAND (1969) の報告した風波のスペクトルの "overshoot" 現象と関連している。ある周波数帯のエネルギーの増大と他の周波数帯のエネルギーの減少とが関連しあっていることを，観測結果は示している。従来の PHILLIPS, MILES, その他による風波の発生と成長の理論では，周波数成分間のエネルギーの交換は考慮されていない。

LONGUET-HIGGINS (1969) の波の成長についての新しい理論と今回の観測値とを比較した。その結果，急速な成長過程において観測されたスペクトル密度 $\Phi(f)$ が，吹走時間 t の関数として: $\Phi(f)=\{r(f)\cdot(t-t_f)\}^2$ の形で表現されることが示された。ここで t_f は周波数によって急速な成長の開始時刻が異なることを示している。LONGUET-HIGGINS の理論は，風波のスペクトル密度の時間変化に特有の overshoot 現象を説明することができない。

スペクトル密度が増加する周波数帯の分布を特長づける3つの周波数を選ぶと，これら3つの周波数に対応する成分波は，いわゆる "wave-wave interactions" の共鳴条件を満足していることが示された。この非線型相互作用は PHILLIPS (1960), LONGUET-HIGGINS (1962), BENNEY (1962) らによって理論的に研究され，実験的にも確かめられている。急速な成長過程で風波のスペクトル密度が吹走時間の2乗に比例すること，平衡に達した後振動すること等が，"wave-wave interations" の結果として説明できる可能性をこの論文で述べた。